Waste Management 36 (2015) 119–129

Contents lists available at ScienceDirect

Waste Management

journal homepage: www.elsevier.com/locate/wasman

Element composition and mineralogical characterisation of air pollution control residue from UK energy-from-waste facilities

Anna Bogush [a], Julia A. Stegemann [a,*], Ian Wood [b], Amitava Roy [c]

[a] Centre for Resource Efficiency & the Environment (CREE), Department of Civil, Environmental & Geomatic Engineering (CEGE), University College London (UCL), Chadwick Building, Gower Street, London WC1E 6BT, UK
[b] Department of Earth Sciences, University College London (UCL), Gower Street, London WC1E 6BT, UK
[c] J. Bennett Johnston, Sr., Center for Advanced Microstructures & Devices, Louisiana State University, 6980 Jefferson Hwy, Baton Rouge, LA 70806, USA

ARTICLE INFO

Article history:
Received 29 May 2014
Accepted 15 November 2014
Available online 22 December 2014

Keywords:
Energy from waste
Waste to energy (WtE)
Air pollution control residue (APC)
Waste characterisation

ABSTRACT

Air pollution control (APC) residues from energy-from-waste (EfW) are alkaline (corrosive) and contain high concentrations of metals, such as zinc and lead, and soluble salts, such as chlorides and sulphates. The EPA 3050B-extractable concentrations of 66 elements, including critical elements of strategic importance for advanced electronics and energy technologies, were determined in eight APC residues from six UK EfW facilities. The concentrations of Ag (6–15 mg/kg) and In (1–13 mg/kg), as well as potential pollutants, especially Zn (0.26–0.73 wt.%), Pb (0.05–0.2 wt.%), As, Cd, Cu, Mo, Sb, Sn and Se were found to be enriched in all APC residues compared to average crustal abundances. Results from a combination of scanning electron microscopy with energy dispersive X-ray spectroscopy and also powder X-ray diffraction, thermal analysis and Fourier transform infrared spectroscopy give an exceptionally full understanding of the mineralogy of these residues, which is discussed in the context of other results in the literature. The present work has shown that the bulk of the crystalline phases present in the investigated APC residues include Ca-based phases, such as $CaCl_xOH_{2-x}$, $CaCO_3$, $Ca(OH)_2$, $CaSO_4$, and CaO, as well as soluble salts, such as NaCl and KCl. Poorly-crystalline aragonite was identified by FTIR. Sulphur appears to have complex redox speciation, presenting as both anhydrite and hannebachite in some UK EfW APC residues. Hazardous elements (Zn and Pb) were widely associated with soluble Ca- and Cl-bearing phases (e.g. $CaCl_xOH_{2-x}$ and sylvite), as well as unburnt organic matter and aluminosilicates. Specific metal-bearing minerals were also detected in some samples: e.g., Pb present as cerussite; Zn in gahnite, zincowoodwardite and copper nickel zinc oxide; Cu in tenorite, copper nickel zinc oxide and fedotovite. Aluminium foil pieces were present and abundantly covered by fine phases, particularly in any cracks, probably in the form of Friedel's salt.

1. Introduction

1.1. Background

Air pollution control (APC) residues from energy-from-waste (EfW) represent only 2–6% of the original volume of the municipal solid waste (MSW). However, APC residues are classified as hazardous wastes because they are alkaline (corrosive) and contain high concentrations of metals (e.g., Pb, Zn, Cd, Cr, Cu, Hg), soluble salts, such as chlorides and sulphates, and toxic organic pollutants (e.g., dioxins and furans) due to volatilisation and condensation processes in the boiler and flue gas cleaning systems (Amutha Rani et al., 2008; Astrup et al., 2005, 2006; BREF, 2006; Chandler et al., 1997; De Boom and Degrez, 2012; Quina et al., 2008b, 2011). They are classified as hazardous wastes under code 19 01 07* in the European Waste Catalogue (EWC, European Commission Decision 2000/532/EC, 2000).

The work described in this paper was undertaken to gain a better understanding of the composition, mineralogy and nature of the host phases which can be responsible for leaching behaviour of potentially dangerous elements in APC residues from UK EfW facilities. A thorough analysis of these aspects is necessary to enable development of the best options to manage this waste. Novel findings from this work with multiple complex methods are discussed in the context of the literature in this area from the past two decades.

* Corresponding author. Tel.: +44 (0)2076797370.
E-mail address: j.stegemann@ucl.ac.uk (J.A. Stegemann).

http://dx.doi.org/10.1016/j.wasman.2014.11.017
0956-053X/

1.2. Formation of APC residues

Flue gases from combustion processes contain fine particles that are entrained as the gas rises through the combustion chamber, known as fly ash, as well as acid gases (hydrogen chloride and sulphur dioxide) and trace quantities of uncombusted or uncombustible volatilised pollutants. APC residues are generated in the flue gas cleaning process. Although various APC schemes exist, commonly flue gases are cooled through heat exchange with water in a boiler and pass to a semi-dry scrubbing system, where acid gases are neutralized by the addition of hydrated lime ($Ca(OH)_2$). An ammonia scrubber may be used for reduction of nitrogen oxides (NOx) and sodium sulphide may be added to remove Hg; alternatively Hg may be removed with activated carbon, together with trace organic pollutants such as dioxins. Scrubbing residues and fly ash particles are then captured together by a fabric filter, producing APC residue (BREF, 2006; Chandler et al., 1997; Quina et al., 2011). In addition to chloride and sulphate captured in flue gas neutralisation, metals are concentrated in APC residues due to volatilisation and condensation processes in the boiler and flue gas cleaning systems (Astrup et al., 2006; Chandler et al., 1997; Song et al., 2004).

The boiling points of different phases (oxides, chlorides, sulphides, etc.) are primary factors which determine the presence of metals in APC residues (Davison et al., 1974; Fernandez et al., 1992). Klein et al. (1975) proposed the following classification of elements in relation to their accumulation (or not) in fly ash, according to their boiling points:

- Class I (e.g., Al, Ba, Ca, Co, Fe, K, Mg, Mn, Si, Sr, and Ti) elements have high boiling points, are not volatilised in the combustion area, but can be entrained as small particles or droplets that form the basis of the fly ash;
- Class II (e.g., As, Cd, Cu, Ga, Pb, Sb, Zn, and Se) elements are volatilised during combustion with subsequent condensation on the surface of the fly ash particles;
- Class III (e.g., Hg, Cl, and Br) elements volatilise and remain in the gas phase throughout the combustion process, but are removed by APC systems;
- Other elements (e.g., Cr, Cs, Na, Ni, U, and V) have mixed behaviour between Classes I and II.

In early work on this subject, Greenberg et al. (1978) assumed formation of chlorides of Pb, Sb, Cd, As, Zn, and Ni, whose boiling points are below 1273 K, in the combustion gas stream. Fernandez et al. (1992) investigated this vital issue in detail and concluded that three different relative stabilities are possible for metal compounds present in the incineration process, depending on the thermodynamic stability of their oxides and chlorides:

(1) If the oxide is more stable than the chloride, an element is transported mechanically and is found in the matrix of the fly ash particles;
(2) Elements whose oxides and chlorides have similar stabilities are transported by both volatilisation-condensation and mechanical mechanisms;
(3) If the chloride is more stable than the oxide, then the metal chloride volatilises and condenses on the surface of the fly ash particles, forming compounds with high solubility.

Fernandez et al. (1992) also showed that the formation-volatilisation-condensation of chlorides plays an important role in the transport of metals by the combustion gas stream. Verhulst et al. (1996) provided more information about elements under the conditions in MSW incinerators based on thermodynamic equilibrium calculations. For example, as temperature increases, solid $ZnCl_2$ converts to solid ZnO at around 280 °C, while $ZnCl_2$ vapour forms concurrently from about 140 °C. $ZnCl_2$ volatilisation increases with temperature, chloride concentration and reducing conditions, reaching about 70% at 800 °C if sufficient chloride is present. By contrast, the boiling point of $FeCl_3$ is approximately 650 °C, but the iron oxides are very stable and no significant amount of Fe is volatilised, even at 1100 °C. These authors also provided information about other elements (Hg, Cd, Pb, Cu, As, Sb, Mn, Mg, Al, Ti, and Sn). Recent work by Zhang et al. (2012) indicates that waste moisture content also influences element speciation. Thus, the presence of elements in specific species and their concentrations in fly ashes and APC residues definitely depends on the type of waste combusted, and its content of chlorine, sulphur and water; the oxidation level (amount of oxygen/(C + H)); temperature, and processing time, as well as boiling points of the different phases.

1.3. Mineralogical characterisation of APC residues

EfW APC residues are complex mixtures of various minerals, some originating from the entrained fly ash, and others imparted by the condensation and other reactions, as well as unreacted reagents, during flue gas cleaning. The morphology and mineralogy of APC residues has been investigated by several researchers (Alba et al., 1997; Bodenan and Deniard, 2003; Chandler et al., 1997; Dimech et al., 2008; Eighmy et al., 1995; Geysen et al., 2004; He et al., 2004; Le Forestier and Libourel, 1998; Li et al., 2004; Stuart and Kosson, 1994; Sun et al., 2008). APC residues may be composed of five types of particles, e.g., fused spheres, crystalline, polycrystalline, opaque and char (Chandler et al., 1997). As was mentioned by Le Forestier and Libourel (1998), APC residue contains unaltered entrained fly ash, reaction products (salts) and surplus reagent (lime). They also indicated that there are a wide range of particle shapes in APC residues, e.g., spheres, flakes, prisms, needles and sintered agglomerations of dust. Aluminosilicates produced from melt droplets during incineration of the municipal solid waste form smooth particles (Bayuseno and Schmahl, 2011; Eighmy et al., 1995; Kirby and Rimstidt, 1993). Char and agglomerated spheres were observed by Stuart and Kosson (1994) in lime spray drier scrubber residues from MSW incineration. The mineral phases previously identified in APC residues by instrumental methods are summarised in Table 1.

2. Materials

Eight APC residue samples were provided from six different UK EfW facilities, which burn predominantly MSW (European Waste Catalogue code 20 03 01) and its fractions, and range in capacity from less than a hundred thousand tonnes per year to several hundred thousand tonnes per year. The facilities are all mass-burn incinerators, with a minimum operating temperature of 850 °C, ammonia or urea injection for NOx abatement, lime injection to remove acid gases, activated carbon addition for sorption of metals and organic compounds, and capture of the APC residue by a fabric filter. The amount of APC residue collected ranged from 2.2–3.2% of the feed. The samples were provided on an anonymous basis and are identified here as A3, A8, A10, 1, 2, 4, 5, and 9. Samples A3, A8 and A10 were obtained from the same facility at different times. The samples were all "dusty" fine-grained powders, with the exception of A10, which had a fine sandy texture. The colour of these samples ranged from white to dark grey. Dark particles observed in the APC residues are likely to be unburnt carbon, whereas white particles are likely to be unreacted hydrated lime particles, injected for acid gas neutralisation. The APC residue moisture content was quite low and varied from 0.42–2.48% wet

Table 1
Mineral phases previously identified in APC residues from combustion of MSW.

Source	Calcite	Anhydrite/bassanite/gypsum	Halite	Sylvite	Calcium chloride hydroxide	Portlandite	Lime	Ettringite	Gibbsite/Corundum	Grossite	Gismondine	Melilite (incl. Gehlenite)	Feldspar	Whitlockite	Chloroapatite	Oldhamite	Quartz	Wollastonite	Larnite	Hematite	Magnetite	Rutile	Perovskite	Zn metal	Zinc oxide/zincite	Zinc chloride	Potassium tetrachlorozincate	Zinc bromide	Zinc oxysulphate	Hemimorphite	Spinel	Lead oxide	Lead chloride	Tetrapotassium lead oxide	Metals & complex alloys	Graphite
	$CaCO_3$	$CaSO_4$·$0.5H_2O$/$CaSO_4$·$2H_2O$	NaCl	KCl	CaClOH	$Ca(OH)_2$	CaO	$Ca_6Al_2(SO_4)_3OH_{12}$·$26H_2O$	$Al(OH)_3$ / Al_2O_3	$CaAl_4O_7$	$CaAl_2Si_2O_8$·$4H_2O$	$Ca_2(Mg,Al)(Al,Si)_2O_7$/ $Ca_2Al[AlSiO_7]$	$KAlSi_3O_8$ – $NaAlSi_3O_8$ –$CaAl_2Si_2O_8$	$Ca_3(PO_4)_2$	$Ca_5(PO_4)_3Cl$	CaS	SiO_2	$CaSiO_3$	Ca_2SiO_4	Fe_2O_3	Fe_3O_4	TiO_2	$CaTiO_3$	Zn	ZnO	$ZnCl_2$	K_2ZnCl_4	$ZnBr_2$	$Zn_3O(SO_4)_2$	$Zn_4Si_2O_7(OH)_2$·$2H_2O$	(Zn, Ni, Fe)Fe_2O_4	PbO	$PbCl_2$	K_4PbO_4	Fe, Al, Zn (Fe-Al-Cu-Ni-Zn-Si-C)	C
Alba et al. (1997)	x	x	x	x	x						x						x																			
Bodenan & Deniard (2003)	x	x	x	x	x																															
Dimech et al. (2008)	x	x	x	x	x	x																														
Eighmy et al. (1995)	x	x	x			x		x	x	x								x						x	x	x	x	x	x	x				x		
Geysen et al. (2004)	x	x	x	x	x	x											x																			
He et al. (2004)	x	x					x					x																				x				
Le Forestier & Libourel (1998)	x							x	x			x	x	x	x			x	x	x	x	x	x	x		x					x	x	x	x	x	x
Li et al. (2004)	x	x	x	x												x	x																			
Quina et al. (2008b)	x	x	x	x	x	x						x					x			x				x	x	x										
Sun et al. (2008)	x	x	x	x	x	x	x										x																			

mass. Since the residues contain hygroscopic phases (Quina et al., 2008b), the samples were stored in air-tight containers.

3. Methods

An approximately 10 kg composite sample of APC residue was obtained from each of the full-scale facilities at a single sampling time by the facility operator. Representative subsamples of the required size for the analyses were obtained for each of the APC residues by coning and quartering The subsamples were ground for analysis using a micronizing mill. $HNO_3/H_2O_2/HCl$ digests for chemical analysis were prepared according to EPA 3050B (1996), which provides an estimate of the "environmentally available" concentrations of elements in the APC residues, though it may not release all elements, e.g., Ag, which forms AgCl, or elements trapped in aluminosilicates. The EPA 3050B digests of the APC residues were analysed by inductively coupled plasma optical emission spectroscopy (ICP-OES) for bulk elements (Al, Ca, Fe, K, Mg, Mn, Na, P, Si and Ti) and ICP-mass spectrometry (ICP-MS) for trace elements (see row labels in Tables 2a–c for full list.). Chloride and sulphate concentrations were measured by ion chromatography (IC) in distilled water extracts of the APC residues, at a liquid-to-solid ratio of 100.

X-ray powder diffraction (XRD) analysis was used to characterise the crystalline phases present in the APC residues. Each sample was side-loaded against a ground-glass surface into a glass-backed aluminium-framed sample holder. Diffraction patterns were measured in Bragg–Brentano reflection geometry using a PANanalytical X'pert PRO high-resolution powder diffractometer. This diffractometer is equipped with a Co anode X-ray tube (run at 40 kV, 30 mA) and an incident beam Ge monochromator, which produces a single Co $K\alpha_1$ line, leading to very sharp diffraction maxima. All patterns were scanned over the range $4° < 2\theta < 110°$ (25.6 Å < d < 1.09 Å). Phase identification was made by search-matching to the International Centre for Diffraction Data (ICDD) database using the PANanalytical proprietary software ("X'Pert HighScore Plus"). Phases were identified on the basis of a minimum of 3 diffraction lines.

Simultaneous thermal analysis measurements were performed with a TA Instruments Q-600 SDT. Runs were conducted using about 20 mg of sample in alumina pans with a nitrogen purge gas flow rate of 100 mL/min, equilibration at 40 °C for 10 min, followed by a heating rate of 5 °C/min from 40 °C to 200 °C, and then a heating rate of 10 °C/min up to 1000 °C.

Fourier transform infrared spectra were obtained with a Thermo-Fischer Scientific Nicolet 670 spectrometer with an attenuated total reflectance (ATR, Smart iTR) attachment. Diamond plates were used in the ATR. The spectra were collected for the range 4000–650 cm^{-1}.

The morphology of the APC residue particles was investigated by scanning electron microscopy (SEM) at different magnifications on a JEOL JSM-6480LV high-performance, variable pressure analytical scanning electron microscope with secondary electron imaging (SEI) and backscattered electron imaging (BEI) detectors. Individual APC residue particles and compacted APC residue samples were mounted rigidly on a specimen stub and coated with an ultrathin layer of carbon (graphite).

Table 2a
Concentrations of major (>0.1%) elements measured in digests of UK EfW APC residues using EPA 3050B (% dry mass).

Element	A3	A8	A10	1	2	4	5	9	Average	CoV (%)	1995[A]	2013[B]	Crust[C]
Al[a]	1.7	1.3	2.9	1.5	0.90	1.6	1.7	0.95	1.5	35	2.1	3.9	8.23
Ca	26	27	22.4	24	27	24	23	32	26	12	4.6	NA	4.15
Fe	0.88	0.72	2.1	0.63	0.70	0.60	0.67	0.65	0.87	57	<0.16	2.4	0.563
K	2.8	2.6	0.92	2.9	3.5	3.4	3.5	2.4	2.8	30	10.9	NA	2.09
Mg	0.61	0.55	0.84	0.59	0.52	0.71	0.71	0.54	0.62	16	<0.11	NA	2.33
Na	2.6	2.5	1.2	2.8	3.4	3.5	3.0	2.9	2.2	25	8.4	NA	2.36
P	0.46	0.38	0.64	0.45	0.33	0.59	0.56	0.20	0.45	33	NA	NA	0.105
Pb	0.17	0.18	0.05	0.14	0.20	0.14	0.12	0.20	0.16	31	2.7	1.3	12.5
Si[a]	0.57	0.40	0.92	<0.04	0.68	0.51	0.49	0.58	0.30	27	3.8	NA	28.2
Ti	0.14	0.14	0.22	0.14	0.11	0.15	0.16	0.14	0.15	21	0.61	NA	0.57
Zn	0.58	0.73	0.26	0.73	0.71	0.71	0.66	0.37	0.59	31	10.4	3.6	0.0070
Cl as Cl^-	16	15	7.0	18	22	19	18	18	17	26	NA	NA	NA
S as SO_4^{2-}	1.3	2.0	1.2	1.0	1.4	1.2	1.4	1.3	1.4	21	NA	NA	NA

NA indicates that a parameter was not available.
CoV = Coefficient of variation, calculated as 100 × standard deviation/average.
[a] As digestion by EPA 3050B does not dissolve all silicates and aluminosilicates, measurements for Al, Si and elements trapped in aluminosilicates may underestimate total concentrations; the insoluble residue remaining after digestion ranged from approximately 10–70%.
[A] Data from Eighmy et al. (1995).
[B] Based on data from Morf et al. (2013).
[C] Average crustal abundance.

Table 2b
Concentrations of minor (2–1000 mg/kg) elements measured in digests of UK EfW APC residues using EPA 3050B (mg/kg dry mass).

Element	A3	A8	A10	1	2	4	5	9	Average	CoV (%)	1995[A]	2013[B]	Crust[C]
Ag	8.9	11	5.5	10	15	9.9	10	9.6	10	27	192	71	0.07
As	23	27	12	25	29	38	21	26	25	30	960	NA	1.8
Ba	346	372	452	318	352	378	387	316	365	12	<2400	2200	425
Bi	9.6	10	13	30	23	110	15	9.1	28	121	NA	97	0.17
Cd	110	190	26	180	190	150	150	37	128	51	1660	450	0.2
Ce	12	9.4	16	9.4	8.6	10	11	8.6	11	21	12.9	NA	60
Co	17	14	26	19	15	16	23	10	17	29	13.3	61	25
Cr	77	82	110	75	83	85	90	58	83	18	494	780	100
Cs	2.6	2.6	0.86	2.7	3.7	2.3	2.9	4.1	2.7	36	13.5	NA	3.0
Cu	420	460	320	430	580	470	500	510	462	16	2200	2600	55
Ga	4.6	4.2	5.8	4.4	4.6	4.3	4.7	4.7	4.7	11	NA	16	14
In	1.8	2.2	0.72	13	2.9	2.2	2.1	1.1	3.2	122	3.23	6.8	0.1
La	8.9	6.7	12	7.3	6.6	8.9	8.8	5.1	8.0	25	4.72	NA	30
Mn	510	530	760	480	450	550	570	270	520	27	448	NA	950
Mo	12	7.3	12	7.4	15	10	9.2	4.8	9.8	35	47.1	41	1.5
Nd	5.5	4.4	6.9	4.0	3.6	3.9	4.8	4.0	4.6	24	<24.7	11	28
Ni	53	36	59	43	33	32	34	21	39	31	69.8	380	75
Rb	42	42	15	45	60	43	50	49	43	30	206	140	90
Sb	330	470	170	370	510	430	420	320	380	29	NA	NA	0.2
Sc	2.0	2.9	2.7	2.2	2.5	2.3	1.8	3.4	2.5	20	2.3	4.7	22
Se	1.3	0.76	<0.5	<0.5	0.85	<0.5	9.6	2.2	2.9	131	17.4	14	0.05
Sn	380	500	150	470	570	400	400	240	390	36	5900	1800	2.0
Sr	450	330	400	300	310	320	340	330	350	15	NA	460	375
V	12	36	19	15	30	12	16	14	19	46	32.5	40	135
W	<6	<6	<6	<6	17	<6	<6	<6	<17	NA	NA	NA	1.5
Y	6.8	5.5	7.3	4.8	5.3	4.9	5.9	5.8	5.8	15	NA	182	33
Zr	37	31	10	34	29	34	34	27	29	29	<600	49	165

Energy-dispersive X-ray spectroscopy (Oxford Instrument INCAx-sight EDS-system) was used for microanalysis of the solid phases viewed by SEM. SEM/EDS analyses were performed with a 15 kV accelerating voltage. Certified standards were used for calibration. Reduction of element detection limits was achieved by using long counting times; typical element detection limits were about 0.1–0.05 wt.%. Element peaks were automatically identified in the EDS spectrum using AutoID, which also provided tools for manual validation of the elements detected. Summation of the determined elemental composition to 100% was verified. Although more than a hundred spot-analyses were performed, the EDS analyses should be considered to be semi-quantitative, particularly as they were performed on flat surfaces of natural samples rather than polished sections.

4. Results and discussion

4.1. Elemental composition

The concentrations of the 66 elements determined in the eight UK EfW APC residues based on digests using EPA 3050B are given in Tables 2–4, divided into major (a), minor (b) and trace (c) elements. The compositions of the eight samples can be seen to be similar, with coefficients of variation usually ranging from 11–57% of the average (apart from Bi, In, Se and Ta). There was a larger variation in composition within the group of three samples from the same facility (A3, A8 and A10), than between the samples from the six different facilities, suggesting that the composition of APC residues is broadly consistent across different facilities, though it

Table 2c
Concentrations of trace (<2 mg/kg) elements measured in digests of UK EfW APC residues using EPA 3050B (mg/kg dry mass).

Element	A3	A8	A10	1	2	4	5	9	Average	CoV (%)	1995[A]	2013[B]	Crust[C]
Au	<1.2	<1.2	<1.2	<1.2	<1.2	<1.2	<1.2	<1.2	<1.2	NA	NA	1.1	0.004
Be	0.36	0.27	0.43	0.26	0.27	0.29	0.35	0.35	0.32	19	NA	0	2.8
Dy	0.8	0.69	0.82	0.53	0.58	0.52	0.64	0.67	0.66	17	<9.75	0	3.0
Er	0.42	0.40	0.50	0.34	0.33	0.31	0.40	0.41	0.39	15	NA	NA	2.8
Eu	0.38	0.27	0.45	0.25	0.25	0.28	0.35	0.29	0.32	22	<0.86	NA	1.2
Gd	1.1	0.91	1.2	0.69	0.72	0.79	0.92	0.86	0.90	20	NA	1.7	5.4
Ge	0.33	0.46	0.66	0.19	0.39	0.20	0.31	0.22	0.34	47	NA	2.3	1.5
Hf	0.87	0.84	0.03	0.74	0.73	0.77	0.78	0.64	0.68	40	1.25	46	3.0
Ho	0.15	0.13	0.16	0.11	0.12	0.097	0.13	0.14	0.13	15	NA	NA	1.2
Ir	<0.2	<0.2	<0.2	<0.2	<0.2	<0.2	<0.2	<0.2	<0.2	NA	NA	NA	NA
Lu	0.058	0.048	0.06	0.04	0.043	0.037	0.05	0.047	0.05	16	NA	NA	0.5
Nb	<0.7	<0.7	<0.7	<0.7	<0.7	<0.7	<0.7	<0.7	<0.7	NA	NA	10	20
Pd	0.58	036	1.1	0.39	0.36	0.30	0.51	<0.28	0.52	54	NA	NA	NA
Pr	1.5	1.2	1.9	1.1	1.0	1.1	1.3	1.0	1.3	24	NA	2.8	8.2
Pt	<0.04	<0.04	0.67	0.041	<0.04	<0.04	<0.04	<0.04	<0.67	NA	NA	0.24	NA
Rh	0.069	0.066	0.032	0.06	0.074	0.06	0.060	0.081	0.06	25	NA	0	NA
Ru	<0.03	<0.03	<0.03	<0.03	<0.03	<0.03	<0.03	<0.03	<0.03	<0.03	NA	0	NA
Sm	1.0	0.86	1.1	0.71	1.2	0.68	0.86	0.76	0.90	21	1.11	NA	6.0
Ta	<0.03	<0.03	<0.03	0.039	0.186	<0.03	<0.03	0.035	0.09	96	<0.87	6	2.0
Tb	0.16	0.13	0.22	0.11	0.11	0.12	0.13	0.14	0.14	21	<0.94	NA	0.9
Te	<0.3	0.42	<0.3	<0.3	<0.3	<0.3	0.28	0.32	0.34	21	NA	2.3	NA
Th	1.5	1.1	2.1	1.2	0.93	1.2	1.5	0.94	1.3	29	<0.2	NA	9.6
Tl	0.24	0.34	<0.2	0.17	0.19	<0.2	0.50	0.30	0.29	41	NA	2.3	0.45
Tm	0.054	0.057	0.060	0.043	0.044	0.043	0.050	0.048	0.05	12	NA	NA	0.48
U	0.63	0.82	0.92	0.87	1.0	0.97	0.92	1.4	0.94	23	<3.05	NA	2.7
Yb	0.41	0.39	0.46	0.34	0.33	0.37	0.38	0.34	0.38	12	<2.4	NA	3.0

may vary over time in each facility. The residue composition generally agrees with other results (Alba et al., 1997; Chandler et al., 1997; De Boom and Degrez, 2012; Hyks et al., 2009; Lampris et al., 2009; Morf et al., 2013; Quina et al., 2008a, 2008b); results obtained by Eighmy et al. (1995) and Morf et al. (2013) are shown for comparison. Lower measurements of some toxic metals in the UK APC residues may reflect use of a higher MSW combustion temperature or more aggressive digestion procedure with hydrofluoric acid by Eighmy et al. (1995) and Morf et al. (2013). Decreases in concentrations of metals that are now less common in consumer goods over time may also be observed (e.g., for Cd). The concentrations can be compared with the average crustal abundances of these elements (Taylor, 1964). Ca was found to be significantly enriched in the APC residues, because excess $Ca(OH)_2$ is used to scrub acid flue gases. Variations in the Ca concentrations between APC residues suggest different $Ca(OH)_2$ additions. The concentrations of potential pollutants, especially Zn and Pb, and also As, Cd, Cu, Mo, Sb, Sn, Se, are enriched in all APC residues. For example, Sb exceeds the average crustal abundance by 240–2500 times, Cd by 20–950 times, Zn by 15–100 times, Pb by 30–160 times, Sn by 6–230 times, and Cu by 3–10 times. APC residues are enriched in the more volatile elements such as Zn, Pb, Cd, and As and contain less lithophilic elements such as Al, Si and Ti, compared to bottom ash. Also, the contents of In and Ag, which are strategically important metals, exceed the average crustal abundance by 7–130 and 79–160 times, respectively. Although they are lower than present ore concentrations (10–20 mg/kg for In, according to Alfantazi and Moskalyk, 2003, and generally much higher for Ag), their value adds attraction to any scheme for extraction of multiple metals from APC residues. Concentrations of rare earth elements, which are less volatile elements, are quite low in comparison with average crustal abundance of these elements and agree well with results for these elements from Eighmy et al. (1995) and Morf et al. (2013).

4.2. X-ray diffraction

The results from XRD to identify the crystalline phases are summarised in Fig. 1. The bulk of the crystalline phases present in the

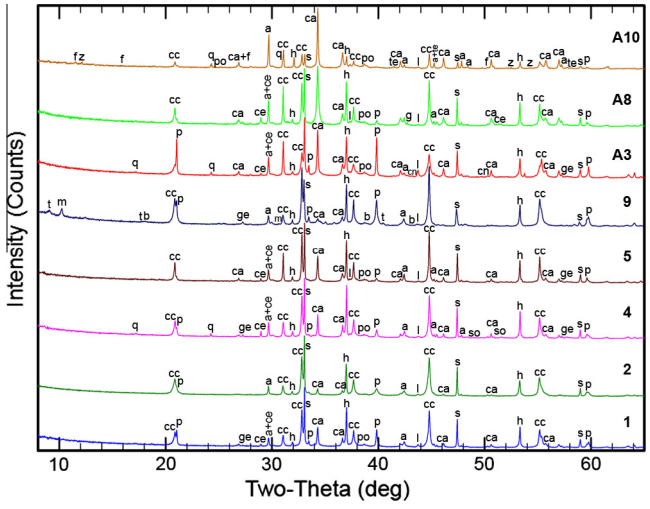

Fig. 1. Mineral phases identified in UK EfW APC residues by XRD. Mineral identification code and chemical formulas: a – anhydrite, $CaSO_4$; b – botallackite, $CuCl_2(Cu(OH)_2)_3$; ca – calcite, $CaCO_3$; cc – calcium chloride hydroxide, CaClOH; ce – cerussite, $PbCO_3$; cn – copper nickel zinc oxide, $Cu_{1.02}ZnNi_{3.27}O_{5.29}$; cs – calcium sulphate hydrate, $CaSO_4{\cdot}H_2O$; f – fedotovite, $K_2Cu_3O(SO_4)_3$; g – gahnite, $ZnAl_2O_4$; ge – gehlenite, $Ca_2Al(AlSiO_7)$; h – halite, NaCl; l – lime, CaO; m – magnesium oxide hydroxide, $MgO_2(OH)_2$; p – portlandite, $Ca(OH)_2$; po – potassium aluminium silicate, $K_{1.25}Al_{1.25}Si_{0.75}O_4$; q – quartz, SiO_2; s – sylvite, KCl; so – sodalite, $Ca_8Al_{12}O_{24}(MoO_4)_2$; t – tobermorite, $Ca_5Si_6O_{16}(OH)_2{\cdot}4H_2O$; te – tenorite, CuO; z – zincowoodwardite, $Zn_{1-x}Al_x(OH)_2(SO_4)_x(H_2O)_n$.

APC residues include Ca-based phases, such as CaClOH, $CaCO_3$, $Ca(OH)_2$, $CaSO_4$, and CaO, as well as soluble salts, such as NaCl and KCl. Crystalline SiO_2, $Ca_2Al(AlSiO_7)$, tobermorite ($Ca_5Si_6O_{16}(OH)_2{\cdot}4H_2O$), magnesium oxide hydroxide ($Mg_3O_2(OH)_2$) were found in several of the APC residues, as well as $K_{1.25}Al_{1.25}Si_{0.75}O_4$. The above phases identified in these eight APC residues from UK EfW facilities are in particular agreement with results from the literature (see Table 1), with the exception of tobermorite, magnesium oxide hydroxide and $K_{1.25}Al_{1.25}Si_{0.75}O_4$, which were not identified before. A large proportion of the crystalline phases present in

the APC residues include Ca-based phases from reaction of the hydrated lime reagent with acid gases, or excess reagent; variations in the contents of CaClOH, $CaCO_3$ and $Ca(OH)_2$ depend mainly on the amount of hydrated lime addition. The content of calcium chloride hydroxide (CaClOH) is quite high in all of the APC residues and might be formed by the interaction of hydrated lime ($Ca(OH)_2$) with HCl in the following reactions (Josewicz and Gullett, 1995):

$$Ca(OH)_2 + 2HCl \rightarrow CaCl_2 + 2H_2O;$$

$$Ca(OH)_2 + HCl \rightarrow CaClOH + H_2O;$$

$$Ca(OH)_2 + CaCl_2 \rightarrow 2CaClOH.$$

Several metal rich mineral phases identified in this investigation of UK EfW APC residues were not identified before: lead was present as cerussite in samples 1, 4, 5, A3 and A8; copper nickel zinc oxide, gahnite, and zincowoodwardite were found as zinc-rich phases in samples A3, A8 and A10, respectively; additionally, the Cu-bearing minerals tenorite (A10), botallackite (9), fedotovite (A10), and copper nickel zinc oxide (A3) were detected.

The XRD diffractograms also show evidence of some amorphous material in APC residues, as indicated by the background around 30–40° 2 and lack of sharp peaks, which could be glass and/or other non-crystalline or poorly crystalline material. Some peaks, for example, the first one in sample 9 for magnesium oxide hydroxide, are quite broad suggesting a poorly crystalline compound. In comparison, a high amount of amorphous material has been found in the literature (e.g., 33–50% glass was found by Le Forestier and Libourel (1998), Bodenan and Deniard (2003), Bayuseno and Schmahl (2011)).

4.3. Thermal analysis

The differential thermogravimetric (DTG) curves of the APC residues can be broadly divided into four regions (Fig. 2): from 40 °C to 300 °C; from 300 °C to about 550 °C; from 550 °C to about 750 °C; and 750 °C and above. Very little weight loss occurs up to 300 °C. As much as 32% mass loss is seen in the APC residues (A3), most of it occurring at temperatures above 750 °C.

The region 300–550 °C shows overlapping breakdown of calcium hydroxide and calcium hydroxychloride. Considering the XRD results, the peak around 380 °C for the DTG curves is likely to be from calcium hydroxide. Whereas the peak for pure, 100%, calcium hydroxide is around 427 °C for the running parameters used in this study, the calcium hydroxide dehydration peak is expected to occur at lower temperature for lower concentrations (Wendlandt, 1986). On this basis, DTG shows calcium hydroxide, sometimes only in trace amounts, to be present in every residue. The amount of calcium hydroxide in APC residue 9 may be as high as 14% and as low as 0.8% in A8. Bodenan and Deniard (2003), in their study of calcium-based sorbents from European waste incinerators, reported very similar phases. Unlike the single-step breakdown observed in their data, calcium hydroxychloride in this work decomposed in several steps. This may be a function of the instrumental parameters used in this study. The region from 550 °C to 750 °C shows the breakdown of calcium carbonate. The region 750 °C and above shows the breakdown of the sulphate phases (Todor, 1976).

4.4. Fourier transform infrared spectroscopy

The regions 4000–3000 cm^{-1} and 1800–650 cm^{-1} are shown for the Fourier transform infrared (FTIR) spectra of the APC residues (Fig. 3). The 3641 cm^{-1} peak belongs to calcium hydroxide, and correlates well with the calcium hydroxide peak seen in the DTG curves (e.g., APC residue 9). The 3569 cm^{-1} peak belongs to calcium hydroxychloride (Bodenan and Deniard, 2003). The ~1410–1418 cm^{-1} peak could belong to calcite, siderite (1410 cm^{-1}) and/or smithsonite (1405 cm^{-1}). The band for calcite-type minerals is often broad, as observed here, depending on particle size and the polarization effect (White, 1974). Also, the 873 cm^{-1} and 712 cm^{-1} peaks suggest that calcite is present in all samples. There is also a good correlation between the calcite peaks in DTG and FTIR (e.g., A8).

The peak shoulder at 1471 cm^{-1} corresponds to the calcium carbonate polymorph aragonite. This type of double band is seen for vaterite, but the presence of the 860 cm^{-1} peak indicates that aragonite is present, instead of vaterite. The 858 cm^{-1} shoulder of aragonite can be definitively identified in samples 9, 2, 1, A3 and A8. FTIR suggests that aragonite is present in almost all APC residues but it was not detected by XRD and TGA, possibly because of its poorly-crystalline nature.

The sulphate peaks at 1155–1151 cm^{-1} and 1115–1109 cm^{-1} correspond well with those of anhydrite (Marel and Beutelspacher, 1976). The 975 cm^{-1} peak is identified as that of calcium sulphite, based on the similar peak of hannebachite ($2CaSO_3 \cdot 2H_2O$ from Hannebacher, Germany, data not shown). Thus sulphur appears to have complex redox speciation in some APC residues.

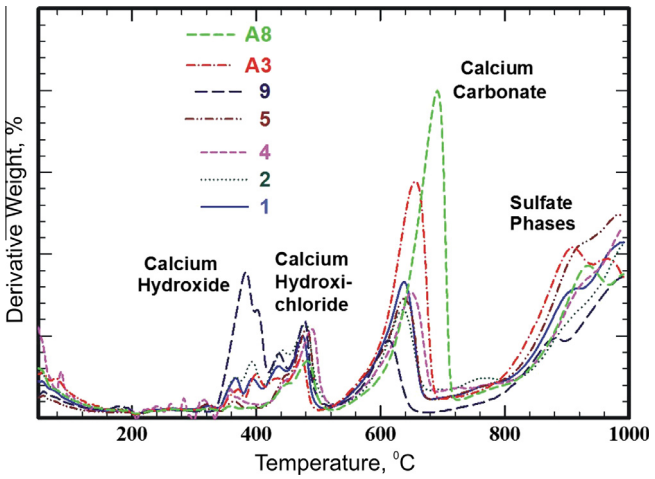

Fig. 2. The differential thermogravimetric curves of UK EfW APC residues.

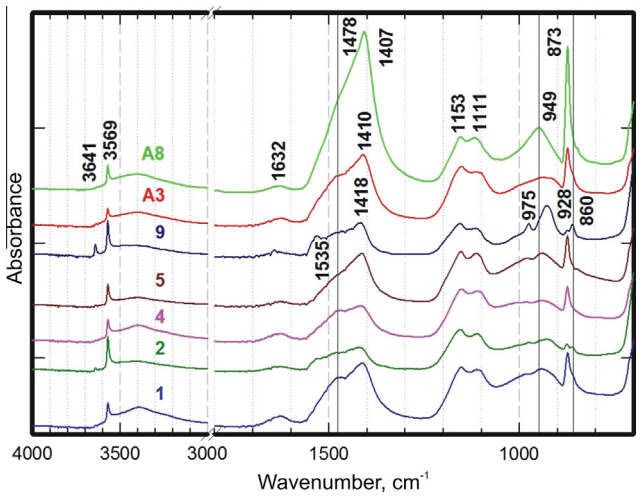

Fig. 3. FTIR spectra of UK EfW APC residues.

4.5. Microstructure and local chemical composition of APC residues by scanning electron microscopy with energy dispersive X-ray spectroscopy

APC residues A10, A8, A3, 1, 2, 4 and 5 mainly contain aggregates, spherical particles, unburnt organic matter, and finer-grained phases. These samples have plenty of spherical particles of different sizes (10–150 μm). The spherical particles are aluminosilicates with impurities of some elements. For example, a calcium aluminosilicate spherical particle from APC residue A10 shown in Fig. 4a contains impurities of Na, Mg, K, S, Cl, Ti, Fe, Cu, Zn and Pb. Spherical Ca(Na, Mg) aluminosilicate particles enriched in Zn (up to 2%), which may be adsorbed on the surface of spherical particles, substituted for Ca and Mg, or, more likely, incorporated in aluminosilicates, were also observed (Fig. 4b, point 1, spectrum 1).

In the APC residues mentioned above, there is a lot of white (based on observation under a light microscope) very fine grained material which consists of Ca, O, Cl as major elements, with impu-

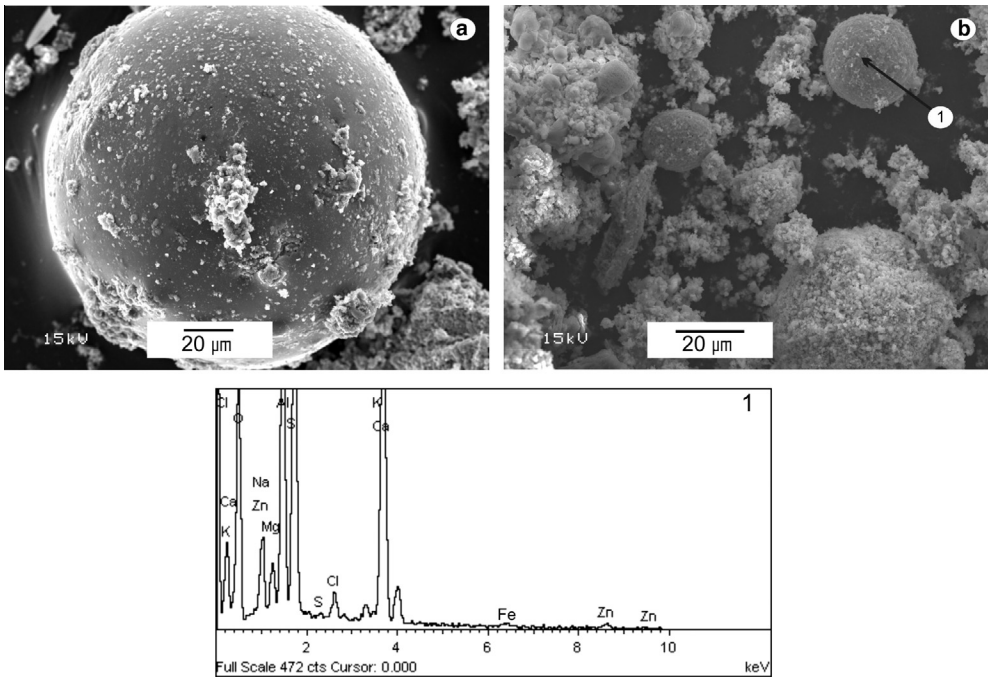

Fig. 4. Scanning electron microscopy images of EfW APC residues: (a) Plain spherical particle from EfW APC residue A10; (b) material from EfW APC residue A3; (1) EDS spectrum of point 1 from b.

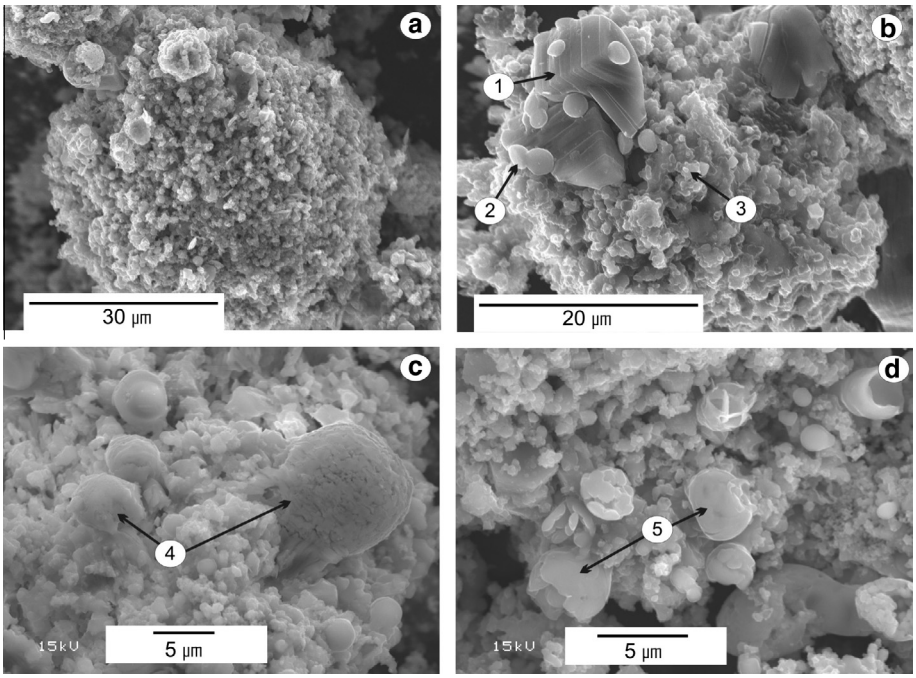

Fig. 5. Scanning electron microscopy images of fine material from EfW APC residues: (a) spherical particle covered by fine phases from EfW APC residue A10; (b) material from EfW APC residue 1; (c) 'mushroom' forms of calcium chloride hydroxide from APC residue A3; (d) residues of cenospheres from APC residue 2.

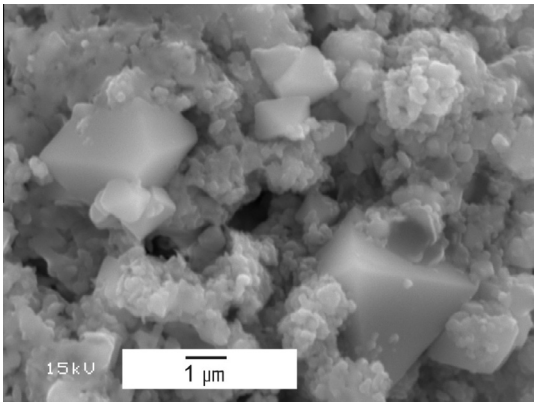

Fig. 6. Scanning electron microscopy image of octahedral crystals from EfW APC residue A3.

rities of K, Na, Si, Al, S, Fe, Zn and Pb (Fig. 5). This fine material is most likely $CaCl_xOH_{2-x}$ (calcium chloride hydroxide), and also covers the majority of the spherical aluminosilicate particles (Fig. 5). $CaCl_xOH_{2-x}$ is a highly soluble phase, which will also release the elements associated with it when it dissolves. The size of these fine particles varies from 0.1 to 0.5 μm. There are different morphological forms of the $CaCl_xOH_{2-x}$ phases, for example, Fig. 5b shows blocks about 10 μm in size (point 1), hemispheres about 1 μm (point 2) and very fine globular particles less than 1 μm (point 3). Fig. 5c (point 4) shows an SEM image of 'mushroom' forms of $CaCl_xOH_{2-x}$ (3–7 μm) which are formed from fine amorphous material with impurities of Fe, Cu, Zn, Sr, and Al. Residues of cenospheres (about 2–7 μm) were found out in A3 and 2 APC residue (Fig. 5d, point 5). They also contain Ca, O and Cl as major elements, probably calcium chloride hydroxide. All these morphological forms of calcium chloride hydroxide concentrate up to 3 wt.% Zn.

Octahedral crystals (2–5 μm, Fig. 6), which were found in all samples, consisted of K and Cl, and are most probably the sylvite detected by XRD. These crystals have impurities of various elements, including Na, Ca, Mg, Al, Si, S, P, Fe and Zn. They, and the elements within them, are likely to be water-soluble. The very fine material surrounding the octahedral crystals again consists of Ca, O and Cl ($CaCl_xOH_{2-x}$) with impurities of K, S, Si, Na, Mg, Pb, Zn, and Fe.

Three types of aggregate were observed in the APC residues (Fig. 7). The first type mainly consists of Ca aluminosilicates with impurities of Cl, K, Na, Mg, S, Fe, and Zn (Fig. 7, point 1). A finer-grained matrix is precipitated on the aggregates with a main phase of $Ca(Na, K)Cl_xOH_{2-x}$, and also contains different elements such as Na, Si, S, Mg, Al, Pb, and Zn. The second type contains fine particles of CaO with impurities of Cl, S, Si, Al, and Zn (Fig. 7, point 2). The third type mainly consists of $CaCl_xOH_{2-x}$ with impurities of Na, K, Mg, Al, Si, S, P, and Zn (Fig. 7, point 3). In detailed investigation of the third aggregate type, it was found to include microspheres (about 5 μm) composed mainly of Mg, Ca, Na, Zn and Si (Fig. 7, point 4), and microparticles of $CaCl_xOH_{2-x}$ with impurities of Na, K, Mg, and Zn (Fig. 7, point 5).

Black flakes in APC residues were found to be unburnt organic matter with a fibrous structure (maybe food, plant, paper or fabric residues, Fig. 8a and b). The unburnt organic matter is associated with P, Na, K, Ca, Mg, Si, Al, S, Cl, Cu, Fe, Zn, Pb, Mo, and Hg. Other phases are deposited on the surface of this organic matter, for example, finer-grained material containing Ca (K, Na) aluminosilicates with impurities of Cl, S, Fe, and Zn (Fig. 8c and d, point (1), and very fine particles of calcium chloride hydroxide with impurities of Na, K, Mg, Si, Al, S, Cl, Fe, and Zn (Fig. 8c, point (2). Other finer-grained phases on the organic matter mainly consist of Ti, O and Ca, probably represent TiO_2 or $CaTiO_3$ phases, with impurities of Mg, K, Si, Al, S, Cl, Fe, and Zn (Fig. 8d, point and EDS spectrum (3).

Aluminium foil pieces were found in the APC residues (Fig. 9a, point (1). Finer-grained phases abundantly precipitate on the surface of the aluminium foils, particularly in any cracks (Fig. 9b, point (2). These phases are mainly composed of Ca, O, Cl, Al, and S with

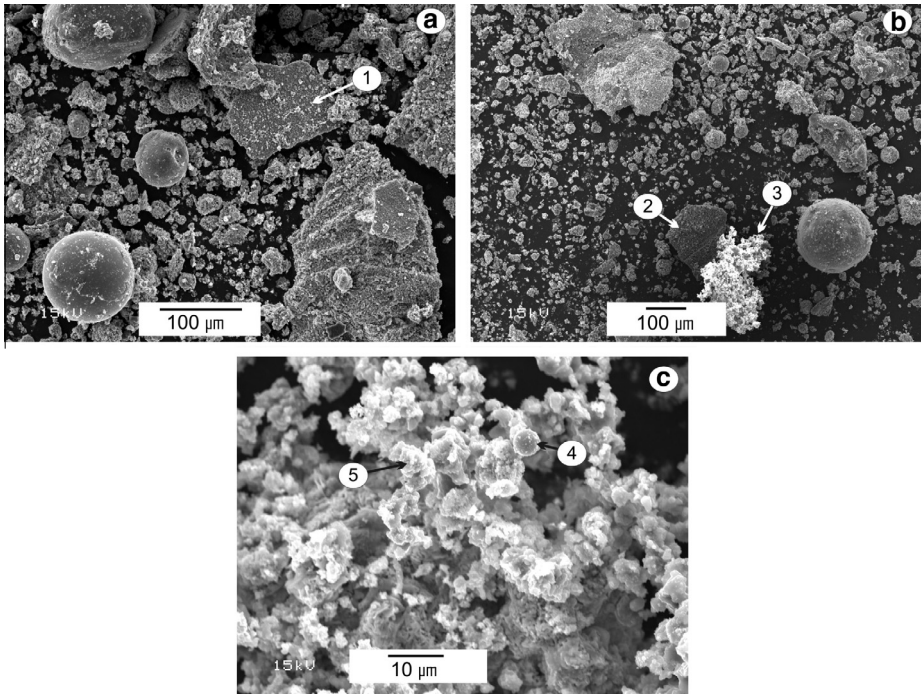

Fig. 7. Scanning electron microscopy images of aggregates from EfW APC residues: (a) in residue 4; (b) and (c) in residue A10.

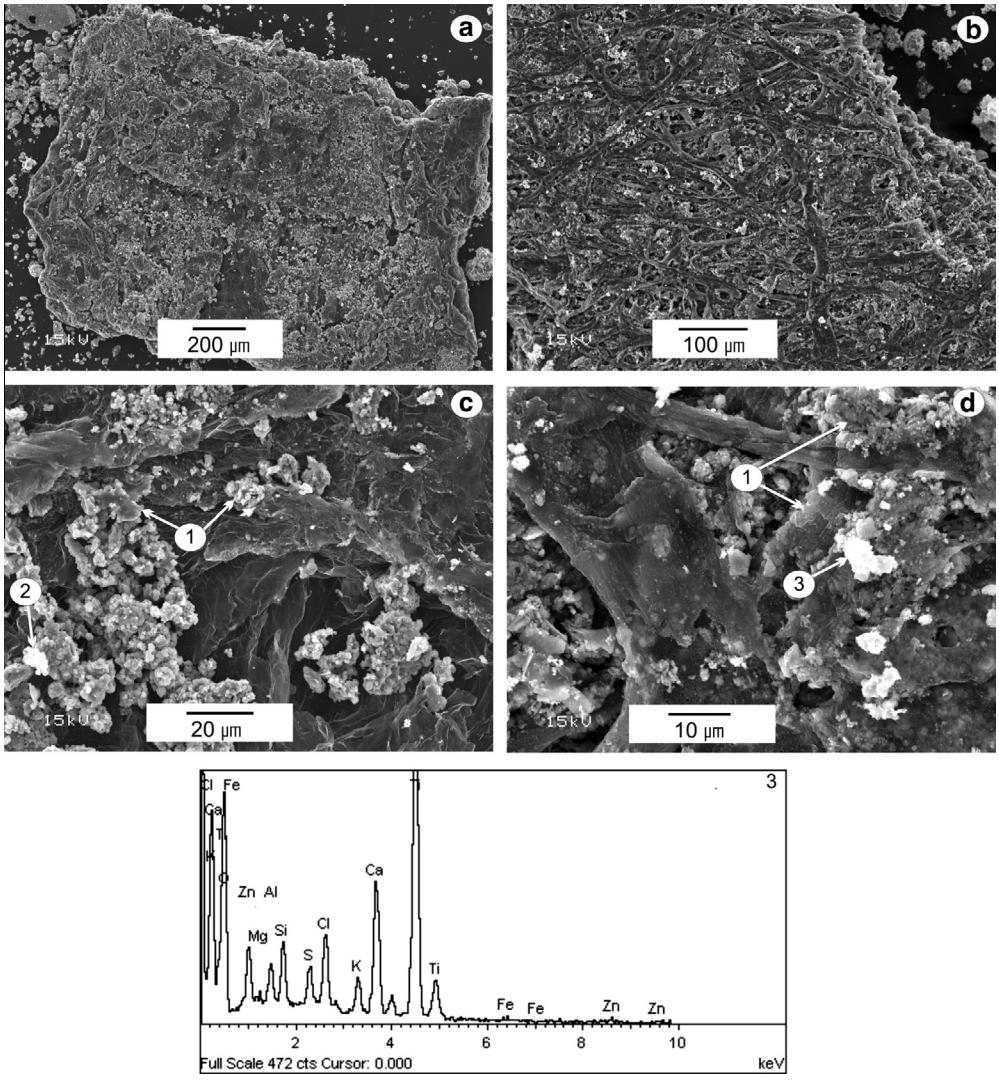

Fig. 8. Scanning electron microscopy images of unburnt organic matter from EfW APC residues: (a) residues of organic matter from EfW APCR A10; (b) unburnt organic material with a fibrous structure from EfW APC residue A3; (c) fine phases deposited on organic matter from A10; (d) fine phases deposited on organic matter from A3; (3) EDS spectrum of point 3 from d.

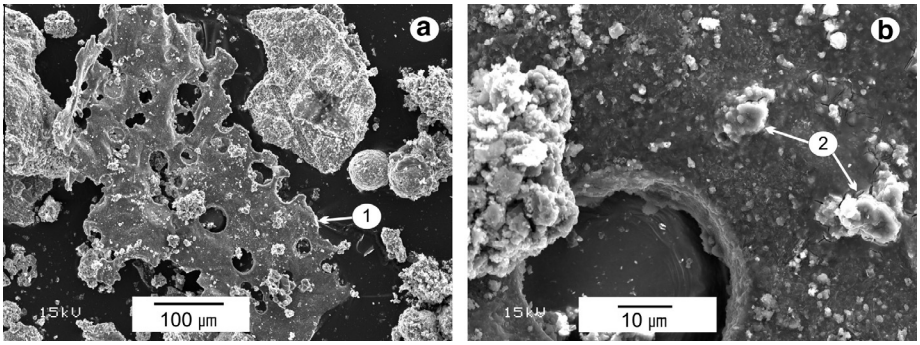

Fig. 9. Scanning electron microscopy images of aluminium foil from EfW APC residues: (a) residue of aluminium foil from EfW APCR A3; (b) fine material on surface and in cracks of aluminium foil from EfW APC residue A3.

impurities of Na, K, Si, P, Fe, Zn and Pb. Probably, the Al foil has corroded and amorphous phases are redeposited on the damaged surface in the form of Friedel's salt ($Ca_2Al(OH)_6[Cl_{1-x}(OH)_x]\cdot 3H_2O$).

APC residue 9 differs from the other APC residues because it contains a lot of very fine material and not many aluminosilicate spheres (Fig. 10). The main phase in this sample is $CaCl_xOH_{2-x}$, which presents in different morphological forms such as powdered finer-grained material (Fig. 10, point (1), flattened hollow spherical particles (point 2) and gel-forming phases (point 3). These phases concentrate different elements such as K, Na, Mg, Si, Al, Fe, Zn, and Pb.

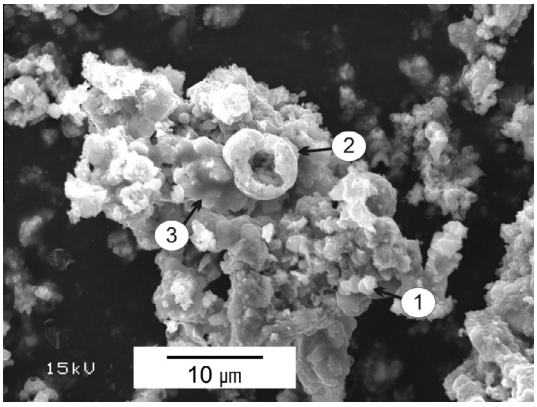

Fig. 10. Scanning electron microscopy image of aggregate from EfW APC residue 9.

5. Conclusions

EfW APC residues are highly complex materials, comprised mainly of Ca, Na, K, Al, Cl^- and SO_4^{2-}, which are found in many minerals. Smaller quantities of other elements can be incorporated in these minerals or adsorbed/deposited on their surfaces. The following phases were found to be present in all the UK EfW APC residues: (1) Ca-bearing phases, such as $CaCl_x(OH)_{2-x}$, calcite ($CaCO_3$), anhydrite ($CaSO_4$), portlandite ($Ca(OH)_2$), lime (CaO), and (2) soluble salts, such as NaCl and KCl. Quartz, gehlenite, calcium sodium aluminium oxide, potassium aluminium silicate, tobermorite and magnesium oxide hydroxide were also found in minor amounts. FTIR suggests that aragonite is definitely present in almost all APC residues except A3, but it is not detected by other techniques (XRD and DTG), possibly because of its poorly-crystalline nature. Sulphur appears to have complex redox speciation, presenting as both anhydrite and hannebachite in some UK EfW APC residues. The presence of some amorphous material in the investigated APC residues was confirmed by XRD (the background around 30–40° 2 and lack of sharp peaks) and FTIR (presence of poorly-crystalline aragonite that was not detected by XRD).

Potential pollutants, especially Zn (0.098–0.73 wt.%) and Pb (0.05–0.2 wt.%), and also As, Cd, Cu, Mo, Sb, Sn, Se, are enriched in all the UK EfW APC residues. They were found to be widely dispersed throughout the residues, although small amounts of metal-rich minerals (cerussite, gahnite, zincowoodwardite, botallackite, copper nickel zinc oxide, tenorite and fedotovite) were detected in some samples.

In general, all the UK APC residues were found to have a similar morphology, being composed of compact spheres and cenospheres of different sizes (2–150 µm) with a smooth texture or covered by finer-grained material. These findings confirm those by previous workers. Moreover, particle size and morphology can be expected to be important in leaching behaviour of elements from APC residue. The spherical particles are aluminosilicates with impurities (e.g., S, Cl, Fe, Cu, Zn and Pb). There are also significant quantities of agglomerated fine phases. This work has shown the fine phases to consist mainly of $CaCl_xOH_{2-x}$ in various morphological forms, including powdered finer-grained material, agglomerated material, cenospheres, 'mushroom' and gel-type phases. These soluble phases were found to be associated with a variety of elements, including Zn, Pb and Cu, and may therefore play a significant role in element leaching. Other soluble phases, such as sylvite were also found to take up Zn and other elements, and can leach them readily. It was also shown that small quantities of unburnt organic matter can concentrate potentially dangerous elements (Zn, Cu, Pb, Hg).

Aluminium foil pieces are also present in EfW APC residues and these are abundantly covered, particularly in any cracks, by finer-grained phases probably in the form of Friedel's salt. Aluminosilicate phases, particularly the spherical particles, also concentrate elements. It is difficult to ascertain by SEM/EDS whether these elements are substituted for Ca and Mg, incorporated interstitially or adsorbed on the surface of the spherical particles. Elements incorporated in silicates or aluminosilicates can be expected to have low solubility, whereas they may be more easily released if they are otherwise incorporated or adsorbed.

Thus, potentially dangerous elements such as Zn and Pb and others, whose boiling temperatures are below the combustion temperature of up to 1500 °C, are volatilised and then may form individual metal-reach phases, condense on the surface of aluminosilicate particles as well as adsorb on or coprecipitate with different phases ($CaCl_xOH_{2-x}$, $Ca(OH)_2$, CaO, etc.).

Acknowledgements

The authors gratefully acknowledge the valuable assistance of the following people:

- Paul Fernee and Peter Chesney of the Environment Agency;
- Jim Davy in the UCL Earth Sciences, for support with the SEM/EDS analysis;
- Kym Jarvis at the UK Natural Environment Research Council ICP facility;
- Judith Zhou and Ian Sturtevant, for support in the UCL CEGE laboratory.

Special thanks are due to Associate Editor Thomas Astrup and the anonymous reviewers for comments, questions and careful and helpful reviews. This work was conducted with funding from the Environment Agency and the UCL Department of Civil, Environmental & Geomatic Engineering.

References

Alba, N., Gassó, S., Lacorte, T., Baldasano, J.M., 1997. Characterization of municipal solid waste incineration residues from facilities with different air pollution control systems. J. Air Waste Manage. Assoc. 47, 1170–1179.

Alfantazi, A.M., Moskalyk, R.R., 2003. Processing of indium: a review. Miner. Eng. 16 (8), 687–694.

Amutha Rani, D., Boccacchini, A.R., Deegan, D., Cheeseman, C.R., 2008. Air pollution control residues from waste incineration: current UK situation and assessment of alternative technologies. Waste Manage. 28 (11), 2279–2292.

Astrup, T., Dijkstra, J.J., Comans, R.J., Van Der Sloot, H., Cristensen, T.H., 2006. Geochemical modeling of leaching from MSWI air-pollution-control residues. Environ. Sci. Technol. 40, 3551–3557.

Astrup, T., Rosenblad, C., Trapp, S., Christensen, T.H., 2005. Chromium release from waste incineration air-pollution-control residues. Environ. Sci. Technol. 39, 3321–3329.

Bayuseno, A.P., Schmahl, W.W., 2011. Characterization of MSWI fly ash through mineralogy and water extraction. Resour. Conserv. Recycl. 55, 524–534.

Bodenan, F., Deniard, P., 2003. Characterization of flue gas cleaning residues from European solid waste incinerators: assessment of various Ca-bearing sorbent processes. Chemosphere 51, 335–347.

BREF, 2006. Integrated pollution prevention and control – reference document on the best available techniques for waste incineration, European Commission.

Chandler, A.J., Eighmy, T.T., Hartlen, J., Hjelmar, O., Kosson, D.S., Sawell, S.E., Van der Sloot, H.A., Vehlow, J. (Eds.), 1997. Municipal Solid Waste Incinerator Residues: Studies in Environmental Science, vol. 67. Elsevier Science B.V., Amsterdam.

Davison, R.L., Natusch, D.F.S., Wallace, J.R., Evans, C.A., 1974. Trace elements in fly ash – dependence of concentration on particle size. Environ. Sci. Technol. 8 (13), 1107–1113.

De Boom, A., Degrez, M., 2012. Belgian MSWI fly ashes and APC residues: a characterisation study. Waste Manage. 32 (6), 1163–1170.

Dimech, C., Cheeseman, C.R., Cook, S., Simon, J., Boccaccini, A.R., 2008. Production of sintered materials from air pollution control residues from waste incineration. J. Mater. Sci. 43, 4143–4151.

Eighmy, T.T., Eusden, J.D., Krzanowski, J.E., Domingo, D.S., Stampfli, D., Martin, J.R., Erickson, P.M., 1995. Comprehensive approach toward understanding element speciation and leaching behaviour in municipal solid waste incineration electrostatic precipitator ash. Environ. Sci. Technol. 29, 629–646.

EPA 3050B, 1996. Acid digestion of sediments, sludges, and soils.

European Commission Decision 2000/532/EC of 3 May 2000 replacing Decision 94/3/EC establishing a list of wastes pursuant to Article 1(a) of Council Directive 75/442/EEC on waste and Council Decision 94/904/EC establishing a list of hazardous waste pursuant to Article 1(4) of Council Directive 91/689/EEC on hazardous waste.

Fernandez, M.A., Marfiner, L., Segarra, M., Garcia, J.C., Espieil, F., 1992. Behavior of heavy metals in the combustion gases of urban waste incinerators. Environ. Sci. Technol. 26, 1040–1047.

Geysen, D., Vandecasteele, C., Juspers, M., Wauters, G., 2004. Comparison of immobilisation of air pollution control residues with cement and with silica. J. Hazard. Mater. 107, 131–143.

Greenberg, R.R., Zoner, W.H., Gordon, G.E., 1978. Composition and size distributions of particles released in refuse incineration. Environ. Sci. Technol. 12 (5), 566–573.

He, P.J., Zhang, H., Zhang, C.G., Lee, D.J., 2004. Characteristics of air pollution control residues of MSW incineration plant in Shanghai. J. Hazard. Mater. 116 (3), 229–237.

Hyks, J., Astrup, T., Christensen, T.H., 2009. Long-term leaching from MSWI air-pollution-control residues: leaching characterization and modelling. J. Hazard. Mater. 162, 80–91.

Josewicz, W., Gullett, B.K., 1995. Reaction mechanisms of dry Ca-based sorbents with gaseous HCl. Ind. Eng. Chem. Res. 34, 607–612.

Kirby, C.S., Rimstidt, J.D., 1993. Mineralogy and surface properties of municipal solid waste ash. Environ. Sci. Technol. 27, 652–660.

Klein, D.H., Andren, A.W., Carter, J.A., Emery, J.F., Feldman, C., Fulkerson, W., Lyon, W.S., Ogle, J.C., Talmi, Y., Van hook, R.I., Bolton, N., 1975. Pathways of thirty-seven trace elements through coal-fired power plant. Environ. Sci. Technol. 9, 973–979.

Lampris, C., Stegemann, J.A., Cheeseman, C.R., 2009. Solidification/stabilisation of air pollution control residues using Portland cement: physical properties and chloride leaching. Waste Manage. 29, 1067–1075.

Le Forestier, L.L., Libourel, G., 1998. Characterization of flue gas residues from municipal solid waste combustors. Environ. Sci. Technol. 32, 2250–2256.

Li, M., Xiang, J., Hu, S., Sun, L., Su, S., Li, P., Sun, X., 2004. Characterization of solid residues from municipal solid waste incinerator. Fuel 83 (10), 1397–1405.

Marel, H.W.V.D., Beutelspacher, H., 1976. Atlas of Infrared Spectroscopy of Clay Minerals and their Admixtures. Elsevier Scientific Publishing Company, Amsterdam.

Morf, L.S., Gloor, R., Haag, O., Haupt, M., Skutan, S., Di Lorenzo, F., Böni, D., 2013. Precious metals and rare earth elements in municipal solid waste – sources and fate in a Swiss incineration plant. Waste Manage. 33, 634–644.

Quina, M.J., Bordado, J.C.M., Quinta-Ferreira, R.M., 2011. Air pollution control in municipal solid waste incinerators. In: Khallaf, M. (Ed.), The Impact of Air Pollution Health, Economy, Environment and Agricultural Sources. InTech, pp. 331–358.

Quina, M.J., Bordado, J.C., Quinta-Ferreira, R.M., 2008a. Treatment and use of air pollution control residues from MSW incineration: an overview. Waste Manage. 28 (11), 2097–2121.

Quina, M.J., Santos, R.C., Bordado, J.C., Quinta-Ferreira, R.M., 2008b. Characterization of air pollution control residues produced in a municipal solid waste incinerator in Portugal. J. Hazard. Mater. 152, 853–869.

Song, G.J., Kim, K.H., Seo, Y.C., Kim, S.C., 2004. Characteristics of ashes from different locations at the MSW incinerator equipped with various air pollution control devices. Waste Manage. 24, 99–106.

Stuart, B.J., Kosson, D.S., 1994. Characterization of municipal waste combustion air pollution control residues as a function of particle size. Combust. Sci. Technol. 101, 527–548.

Sun, J., Bertosa, M.F., Simons, S.J.R., 2008. Kinetic study of accelerated carbonation of municipal solid waste incinerator air pollution control residues for sequestration of flue gas CO_2. Energy Environ. Sci. 1, 370–377.

Taylor, S.R., 1964. Abundance of chemical elements in the continental crust: a new table. Geochim. et Cosmochim. Acta 28, 1273–1285.

Todor, D.N., 1976. Thermal Analysis of Minerals. Abacus Press, Tunbridge Wells.

Verhulst, D., Buekens, A., Spencer, P.J., Eriksson, G., 1996. Thermodynamic behaviour of metal chlorides and sulphates under the conditions of incineration furnaces. Environ. Sci. Technol. 30, 50–56.

Wendlandt, W.W., 1986. Thermal Analysis. John Wiley & Sons, New York.

White, W.B., 1974. The carbonate minerals. In: Farmer, V.C. (Ed.), The Infrared Spectra of Minerals. Mineralogical Society, London, pp. 227–284.

Zhang, Y.G., Li, Q.H., Jia, J.Y., Meng, A.H., 2012. Thermodynamic analysis on heavy metals partitioning impacted by moisture during the MSW incineration. Waste Manage. 32 (12), 2278–2286.